ELSEVIER

Journal of Organometallic Chemistry 637–639 (2001) 398–406

Journal of Organometallic Chemistry

www.elsevier.com/locate/jorganchem

# Synthesis and characterization of ferrocene-labeled oligodeoxynucleotides

Amy E. Beilstein, Mark W. Grinstaff *,[1]

*Department of Chemistry, Paul M. Gross Chemical Laboratory, Duke University, Durham, NC 27708, USA*

Received 18 January 2001; received in revised form 14 March 2001; accepted 20 March 2001

**Abstract**

Using a facile on-column derivatization procedure, oligodeoxynucleotides (ODNs) are labeled with a ferrocene derivative at specific sites. A Sonagashira cross-coupling reaction, using $Pd(PPh_3)_4$ and CuI, links ferrocene propargylamide to a halogenated base, such as 2′-deoxy-5-iodouridine or 8-bromo-2′-deoxyadenosine, which has been previously incorporated in the ODN strand. The structure and stability of the DNA duplex are not significantly altered after site-specific labeling with ferrocene, as demonstrated by $T_m$ and CD spectroscopy. © 2001 Elsevier Science B.V. All rights reserved.

*Keywords:* Ferrocene; Oligodeoxynucleotides; On-column; Solid-phase; Cross-coupling; Synthesis; Bioorganometallic chemistry

## 1. Introduction

Oligodeoxynucleotides are the focus of many therapeutic and diagnostic applications, as well as fundamental structure, function, and physical studies [1–21]. Since oligodeoxynucleotides (ODNs) do not possess chemical functional groups for detection, there is demand for ODNs labeled with photochemical or electroactive probes. Current oligodeoxynucleotide labels range from metal complexes [4,6,22] to organic dyes [23] that are covalently attached to ODNs either at the ribose [18,24,25], phosphate [26–30], or nucleobase moieties [1,31–38]. In particular, transition metals are ideal markers, due to their photochemical and electrochemical activity, which can be optimized for a specific application. Ferrocene is selected as a label for biomolecules since it is a small, neutral metal complex possessing reversible and tunable redox properties. In fact, ferrocene labels have been covalently linked to DNA oligomers [37,39–42], peptide nucleic acids [43,44], and amino acids [45–47] for electron-transfer and diagnostic studies.

Previous synthetic strategies toward metallo-labeled oligonucleotides have included post-modification of a single strand with the metal complex and preparation of a metallo-labeled phosphoramidite that is incorporated during automated solid-phase DNA synthesis [6]. Post-modification often results in low yield and lengthy purification steps, due to side reactions with the unprotected functional groups on a DNA strand. The phosphoramidite approach permits fewer side reactions, higher yields, and reduced purification steps. However, multiple synthesis and purification steps are often required to synthesize the desired phosphoramidite. Thus, an alternative method for labeling ODNs has been developed [35,37]. This method couples an alkyne functionalized ferrocene derivative to a solid-phase bound ODN containing a halogenated nucleoside. The ODN remains protected during the efficient Pd (0)-catalyzed Sonagashira coupling reaction [48], reducing unwanted side reactions and requiring less purification. Herein we describe the synthesis and characterization of novel oligodeoxynucleotides labeled with ferrocene at either a uridine or adenosine nucleobase. Furthermore, we compare this procedure to the analogous phosphoramidite approach for incorporating ferrocene in oligodeoxynucleotides.

* Corresponding author. Fax: +1-919-660-1605.
*E-mail address:* mwg@chem.duke.edu (M.W. Grinstaff).
[1] http://www.chem.duke.edu/~mwg


PII: S0022-328X(01)00943-3

## 2. Experimental

Reagents were purchased from Aldrich or Acros as highest purity grades and used without further purification. All solvents were freshly distilled under inert atmosphere prior to use unless otherwise noted. Dichloromethane and MeCN were distilled from $CaH_2$. Ethyl ether and THF were distilled from sodium–benzophenone ketyl. Anhydrous DMF was obtained from Aldrich. Reagents for DNA synthesis were purchased from Glen Research. Reversed-phase HPLC was performed on a Rainin HPLC with a C18 column monitoring at 254. Absorption spectra and melting curves were measured on an HP8453 diode array spectrometer. Electrochemical measurements were performed using an EG&G Princeton Applied Research electrochemical apparatus. CD spectra were recorded on a JASCO J-710 Spectropolarimeter. NMR Spectra were recorded on a spectrometer operating at 400 MHz. DNA synthesis was performed on an ABI 395 DNA synthesizer. Fast atom bombardment mass spectra (FABMS) were obtained on a JEOL JMS-SX102A spectrometer using a 3-nitrobenzyl alcohol matrix.

Abbreviations: DCC, dicyclohexylcarbodiimide; HOBt, 1-hydroxybenzotriazole; TEA, triethylamine; DIEA, *N*,*N*-diisopropylethylamine; TMDPSi, *t*-butyldiphenylsilane; DMF, dimethylformamide; TBAF, tetrabutylammonium fluoride; THF, tetrahydrofuran; DMT, dimethoxytrityl; DCU, dicyclohexylurea; DCM, dichloromethane; MeCN, acetonitrile; EtOAc, ethylacetate; MeOH, methanol; Py, pyridine; AcONa, sodium acetate.

### 2.1. Syntheses

#### 2.1.1. Ferrocenoyl propargylamide (FPA, **2**)

Ferrocene carboxylic acid (0.230 g, 1 mmol), propargylamine hydrochloride (0.092 g, 1 mmol), and HOBt (0.153 g, 1 mmol) were dissolved in DMF–$CHCl_3$ (50:50, dry). TEA (0.2 ml, 1.2 mmol) was added to the mixture. The mixture was stirred at 0 °C while DCC (0.248 g, 1.2 mmol) in DMF was then added dropwise. After 12 h at ambient temperature, solvent was removed in vacuo and the brown solid was dissolved in EtOAc. Urea was removed by filtration and the filtrate was washed with 5% $NaHCO_3$, 0.5 N HCl, and water and subsequently dried over sodium sulfate. The solvent was removed in vacuo. The crude product was purified on a silica gel column in $CHCl_3$. Removal of solvent in vacuo afforded 0.250 g of a yellow–orange powder (94% yield). $^1$H-NMR ($CDCl_3$, $\delta$ ppm): 3.1 (1H, s, C*H*); 3.9 (2H, d, C$H_2$); 4.2 (5H, s, unsubstituted Cp ring); 4.35 (2H, t, *m*-*H* on Cp ring); 4.8 (2H, t, *o*-*H* on Cp ring); 8.1 (1H, t, N*H*). HR FAB-MS: Found, 267.0341. Calculated for $C_{14}H_{13}ONFe$, 267.0347.

#### 2.1.2. 2′-Deoxy-5′-dimethoxytrityl-5-ferrocenoylpropargylamide uridine, 5′-DMT-U$^{FPA}$ (**4**)

A solution of **2** (0.5517 g, 2 mmol), **3** (0.6564, 1 mmol), $Pd(PPh_3)_4$, (0.1156 g, 0.1 mmol) and CuI (0.0381 g, 0.2 mmol) was prepared in 60 ml dry DMF. TEA (97 μl) was added to the mixture. After 24 h, the solvent was removed in vacuo and the brown residue was dissolved in $CHCl_3$ and washed with water. The volume of the solution was reduced to 2 ml and then was precipitated from ether. The filtrate was then dried to give a yellow powder (0.756 g; 95% yield). $^1$H-NMR ($CD_3CN$, $\delta$ ppm): 2.28 (m, 2H, 2′ protons); 3.24 (m, 2H, 5′); 3.72 (s, 6H, 2 Me); 3.98 (m, 1H, 4′); 4.14 (s, 5H, Cp, unsubstituted); 4.32 (t, 2H, Cp, *m*); 4.44 (m, 1H, 3′); 4.68 (t, 2H, Cp, *o*); 5.11 (bs, 1H, 3′ O*H*); 6.15 (t, 1H, 1′); 6.85–7.46 (m, 13H, DMT protons); 8.01 (s, 1H, C$^1$*H*). HR FAB-MS: Found, 795.2261. Calculated for $C_{44}H_{41}FeO_8N_3$, 795.2243.

#### 2.1.3. 2′-Deoxy-5′-dimethoxytrityl-3′-phosphoramidite-5-ferrocenoylpropargylamide uridine (**5**)

5′-DMT-U$^{FPA}$ (0.50 g, 0.63 mmol) was azeotroped from Py twice and then dissolved in 15 ml THF. While in inert atmosphere, DIEA (0.53 ml, 3.0 mmol) and 0.26 ml (1.1 mmol) β-cyanoethylchloro-*N*,*N*-diisopropylphosphoramidite were added to the flask with stirring. The mixture was allowed to stir for 30 min, and then the solvent was removed by rotary evaporation. The crude solid was purified on a silica gel column in MeOH–TEA–DCM (5:3:92) to afford the product (0.54 g; 86% yield). $^{31}$P-NMR ($CDCl)_3$ indicated chemical shifts at 149.98 and 149.11 ppm, confirming the nucleoside phosphoramidite.

#### 2.1.4. Ferrocenoyl butanolamide (**7**)

0.500 g (1.53 mmol) of silyl-protected butanolamine, 0.2872 g (1.25 mmol) of ferrocene monocarboxylic acid, 0.260 g of DCC and 0.20 g of HOBt were dissolved in THF–DMF (1:1). TEA (0.5 ml) was added to the mixture. After 15 h, the solvent was removed. Next, the solid was dissolved in $CH_2Cl_2$, and washed with 0.5 M HCl and water. The organic layer was dried over sodium sulfate and then the solvent was removed via rotary evaporation. The resulting residue was dissolved in cold ether to remove more DCU by filtration. The filtrate was dried to give crude product (0.852 g; 96% yield). Next, the residue was dissolved in 30 ml THF and 0.62 g of TBAF (2 mmol) was added. The mixture was stirred at RT for 1.5 h and then the temperature was increased to 50 °C. After the solvent was removed via rotary evaporation, the product was purified by column chromatography (silica gel, $CHCl_3$ to 2% MeOH) (95% yield). $^1$H-NMR ($CDCl_3$, $\delta$ ppm): 1.63 (m, 4H, $NHCH_2(CH_2)_2CH_2OH$); 3.36 (q, 2H, $NHCH_2$); 3.69 (t, 2H, $CH_2OH$); 4.14 (s, 5H, Cp, unsubstituted); 4.29 (t, 2H, Cp, *m*); 4.64 (t, 2H, Cp, *o*); 4.41 (bs, 1H, O*H*); 6.25 (bs, 1H, N*H*). HR FAB-MS: Found, 301.0780. Calc. for $C_{15}H_{19}FeNO_2$, 301.0765.

*2.1.5. Ferrocenoyl butanolamide phosphoramidite (**8**)*

Following a published procedure from a German Patent [49], ferrocenoylbutanolamide (0.100 g, 0.33 mmol) was azeotroped from dry Py. The solid was then dissolved in 5 ml THF and 0.23 ml (1.32 mmol) of DIEA was added. Next, 0.12 ml (0.50 mmol) of β-cyanoethylchloro-*N*,*N*-diisopropylphosphoramidite was added and the mixture was stirred for 15 min. Water (33 μl) was added to the flask and the mixture was stirred for an additional 30 min. Ether–TEA was added to the mixture, causing a yellow precipitate to form and then 15 ml of 10% sodium bicarbonate was added, dissolving the precipitate. The mixture was extracted and then washed twice with water. The organic layer was dried over sodium sulfate, then filtered and dried by rotary evaporation. $^{31}$P-NMR ($CDCl_3$) indicates a peak at 148.46 ppm.

*2.1.6. 5′-O-Methanesulfonyl-thymidine (**10**)*

The reaction was based on a literature procedure [50]. Thymidine **9** (1.53 g, 6.3 mmol) was dissolved in 10 ml of dry Py and cooled to −10 °C. Next, methanesulfonyl chloride (0.5 ml dissolved in 3 ml DCM) was added dropwise over a period of 20 min. The reaction mixture was then kept at 0 °C. After 16 h, 10 ml of MeOH was added to quench the reaction and the solvents were evaporated via high vacuum. The resulting crude product was checked by TLC and purified by column chromatography (silica gel, $CH_3OH$–$CHCl_3$ (1:19)). A white, powdered solid **10** was obtained (1.101 g; 55% yield). $^1$H-NMR ($Me_2SO$, $\delta$ ppm): 1.78 (s, 3H, 5-methyl); 2.08–2.22 (m, 2H, C2′); 3.22 (s, 3H, $CH_3S$); 3.98 (q, 1H, C4′); 4.28 (m, 1H, C3′); 4.40 (m, 2H, C5′); 5.50 (s, 1H, 3′-OH); 6.22 (t, 1H, C1′); 7.48 (s, 1H, C6); 11.25 (s, 1H, N3). FAB-MS: $m/z$: $[M+H]^+$ 321.

*2.1.7. 5′-Azido-5′-deoxythymidine (**11**)*

A solution of **10** (1.00 g, 3.125 mmol) in 20 ml of DMF containing lithium azide (0.555 g, 11.3 mmol) was stirred at 90 °C under nitrogen. After 3 h, the solvent was removed under vacuum. The resulting crude product was purified by column chromatography (silica gel, $CH_3OH$–$CHCl_3$ (1:19)) to afford **11** (0.626 g; 75% yield). $^1$H-NMR ($Me_2SO$, $\delta$ ppm): 1.78 (s, 3H, 5-methyl); 2.08–2.22 (m, 2H, C2′); 3.57 (d, 2H, C5′); 3.85 (q, 1H, C4′); 4.20 (m, 1H, C3′); 5.50 (s, 1H, 3′-OH); 6.22 (t, 1H, C1′); 7.48 (s, 1H, C6); 11.25 (s, 1H, N3). FAB-MS: $m/z$: $[M+H]^+$ 268.

*2.1.8. 5′-Amino-5′-deoxythymidine (**12**)*

To a solution of 5′-azidothymidine (**11**), (0.6258 g, 2.2 mmol) in 30 ml MeOH was added an excess of 10% Pd/C. $H_2$ (g) was bubbled through the mixture at 1 atm for 4 h. The mixture was then filtered through Celite to remove Pd/C and the filtrate was dried by rotary evaporation to yield 0.222 g solid (40% yield). $^1$H-NMR ($Me_2SO$, $\delta$ ppm): 1.78 (s, 3H, 5-methyl); 2.08–2.18 (m, 2H, C2′); 2.75 (s, 2H, amine); 3.37 (s, 2H, C5′); 3.75 (q, 1H, C4′); 4.20 (m, 1H, C3′); 5.20 (s, 1H, 3′-OH); 6.20 (t, 1H, C1′); 7.68 (s, 1H, C6). FAB-MS: $m/z$: $[M+H]$ 242.

*2.1.9. N-Ferrocenoyl-5′-amido-5′-deoxythymidine (**13**)*

A solution of 0.220 g (0.913 mmol) of **12**, 0.230 g (1 mmol) of **1**, 0.135 g of HOBt (1 mmol), and 0.210 g of DCC (1.03 mmol) in 25 ml dry DMF was prepared. TEA (0.14 ml) was added to the solution. After 12 h, DCM was added and the mixture was filtered to remove a yellow solid from the red–orange filtrate. The yellow powder was dissolved in 50 ml THF and chilled in an ice bath for 2 h, then filtered to remove urea. The resulting filtrate was dried to yield a red solid, which was purified by column chromatography (40% yield). $^1$H-NMR (ACN, $\delta$ ppm)1.85 (s, 3H, Me); 2.20 (t, 2H, 2′ protons); 3.45–3.62 (m, 1H, 5′ protons); 3.94 (m, 1H, 4′ proton); 4.16 (s, 5H, Cp ring, unsubstituted); 4.29 (m, 1H, 3′ proton); 4.35 (t, 2H, Cp, *m*); 4.72 (t, 2H, Cp, *o*); 6.13 (t, 1H, 1′ proton); 6.86 (bs, 1H, N*H*); 7.41 (s, 1H, C$^6$*H*); 9.30 (s, 1H, N$^3$*H*). ESI MS: Found, 453.22. Calculated for $C_{21}H_{23}FeN_3O_5$, 453.3.

*2.1.10. N-ferrocenoyl-5′-amido-5′-deoxythymidine-3′-phosphoramidite (**14**)*

A solution of 0.095 g (0.2 mmol) of **13** was azeotroped from Py twice. DIEA (0.14 ml, 0.8 mmol) and 3 ml of THF were added to the flask. Once dissolved, 70 μl (0.31 mmol) of β-cyanoethylchloro-*N*,*N*-diisopropylphosphoramidite was added. The mixture was stirred until the solution lost turbidity ($\sim$15 min). The solvent was removed in vacuo. $^{31}$P-NMR ($CD_3CN$) indicated chemical shifts at 150.6 and 149.5 ppm, corresponding to the nucleoside phosphoramidite.

*2.2. Oligodeoxynucleotide syntheses*

*2.2.1. On-column derivatization*

Syntheses were conducted on the 1.0 μM scale. Standard automated DNA synthesis was performed from the 3′- to 5′-terminus until a halogenated nucleoside (8-bromoadenosine or 5-iodouridine) was incorporated. The synthesis was interrupted prior to cleavage of the 5′-dimethoxytrityl group, leaving the ODN bound to the column. $N_2$ was blown through the column for 15 min to dry the column. Next, the column was uncapped and 20 mg FPA, 10 mg $Pd(PPh_3)_4$, and 1 mg CuI were added with 30% TEA in DMF. With closed stopcocks on each end of the column, the column was sealed and was shaken on a hand-shaker for 6 h. The column was then rinsed by pushing through 10 ml of the TEA–DMF mixture, then 50 ml of MeCN. The column was dried for 15 min under $N_2$. Finally, the column was placed back on the synthesizer and standard automated

synthesis was resumed until the desired sequence has been synthesized. After synthesis, the labeled oligomers (with the 5′-DMT removed) were cleaved from the column.

### 2.2.2. Conventional DNA synthesis with ferrocene phosphoramidites

Oligodeoxynucleotide syntheses were performed on a commercial ABI 395 DNA synthesizer from the 3′- to 5′-end using standard automated DNA synthesis protocols as shown in Scheme 5 (1.0 μmol scale). A 0.1 M solution of **5**, **8**, or **14** in dry MeCN was prepared and installed on the DNA synthesizer in a standard reagent bottle. Normal solid-phase oligodeoxynucleotide synthesis was performed. The ferrocene-modified phosphoramidite was introduced and allowed to react with the oligodeoxynucleotide for 15 min. The ferrocene-labeled oligodeoxynucleotides were cleaved from the column and deprotected in 30% $NH_4OH$ at 55 °C for 16 h.

### 2.3. HPLC purification of the oligodeoxynucleotides

HPLC purification of the ferrocene-labeled oligodeoxynucleotides was accomplished on a Rainin HPLC instrument. The crude deprotected oligomers were purified by reverse phase HPLC (Dynamax 300 Å C-18 column [25 cm × 4.6 mm]; 0.1 M TEAA–ACN; 5–25% over 25 min), with labeled oligomers eluting several minutes after non-labeled strands. MALDI or ESI mass spectrometry of the ferrocene-oligodeoxynucleotides confirmed their formation.

### 2.4. Enzymatic digestion

After HPLC purification, labeled oligomers were stored in DI water at −40 °C. Concentrations of these stock solutions were determined by enzymatic degradation (*Penicillium citrinum*, Pharmacia). The oligomer (5 μl), enzyme solution (1 μl), and 44 μl of AcONa buffer were incubated at 60 °C for 30 min, then the absorbance was measured at 260 nm. Extinction coefficients of the strands were calculated by adding the extinction coefficients of each nucleoside in the sequence.

### 2.5. Thermal denaturation

The stability of the ferrocene-labeled duplexes was evaluated by thermal denaturation experiments. A 2.00 μM solution of the duplex in 5 mM sodium phosphate, 50 mM NaCl buffer, pH 7.0, was prepared by mixing appropriate amounts of the complementary single strands (determined by absorbance after enzyme degradation). The mixture was heated to 70 °C for 20 min, then slowly cooled to ambient temperature over 6 h to promote annealing. Thermal denaturation was monitored at 260 nm with a temperature range of 20–70 °C; temperature step, 0.5 °C; integration time, 2 s; and wait time, 2 min. The melting temperature, $T_m$, was determined from the first derivative of the melting profile. Melting temperature averages were obtained from three separate measurements.

### 2.6. Circular dichroism spectroscopy

CD spectra of 2.0 μM solutions of duplexes in phosphate buffer were recorded at 25 °C. Five scans were accumulated for each sample, with a scan rate of 5 nm $s^{-1}$. Data was collected in 5 nm increments.

### 2.7. Cyclic voltammetry

Cyclic voltammetry was performed on an EG&G Princeton Applied Research electrochemical apparatus using a glassy carbon working electrode (3.0 mm diameter), platinum wire auxiliary electrode, and a $Ag \mid Ag^+$ reference electrode. Sample for analysis were dissolved in a solution of $CH_2Cl_2$ containing 0.1 M tetrabutylammonium hexafluorophosphate as the supporting electrolyte at a concentration of 1.0 mM. The scan rate was 100 mV $s^{-1}$ and the data were collected 5 mV increments.

## 3. Results and discussion

In order to capitalize on both the ease of solid-phase DNA synthesis and the efficiency of the Pd (0)-catalyzed Sonagashira reaction, we require a redox probe that is: (1) stable to the standard oligonucleotide syntheses and deprotection reactions; (2) sufficiently soluble as to react with the column-bound halonucleoside in DMF–TEA in the presence of the palladium catalyst; and (3) amenable to covalent attachment to both purine and pyrimidine nucleosides. Ferrocene possess all of these attributes. Furthermore, the labeling site (5-position of uridine or 8-position of adenosine) is chosen so as not to interrupt Watson–Crick base-pairing selectivity [51].

As shown in Scheme 1, the ferrocene precursor for *on-column derivatization* (ferrocenoyl propargylamide

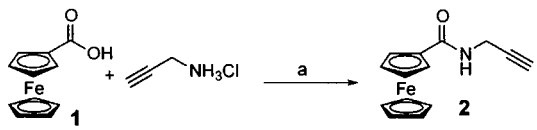


key: (a) DCC, HOBt, TEA, DMF 94% yield.

Scheme 1. Synthesis of the ferrocene precursor, **2**.

or FPA, **2**), was synthesized by coupling ferrocene monocarboxylic acid to propargylamine HCl in the presence of DCC (94% yield). The halonucleoside phosphoramidite precursors, 2′-deoxy-5-iodouridine (5-IdU) and or 8-bromo-2′-deoxyadenosine (8-BrdA) phosphoramidites, required for subsequent Pd(0) cross coupling on-column, were purchased from Glen Research and used without further purification. Automated ODN synthesis was performed on an ABI 395 DNA synthesizer using a standard protocol. The 2′-deoxy-5-iodo-uridine (5-IdU) or 8-bromo-2′-deoxyadenosine (8-BrdA) phosphoramidite was incorporated at the desired position on the ODN (Scheme 2). Phosphoramidite couplings for the standard bases, dA, dC, dG, and dT, as well as 5-IdU and 8-BrdA, were $>95\%$. ODN synthesis was then paused, and the column was removed from the synthesizer and dried with nitrogen gas. The ferrocene precursor, FPA, **2**, (20 mg), $Pd(PPh_3)_4$ (10 mg), and CuI (1 mg) were added to the column, which was then filled with DMF–TEA (9:1). The column was sealed and shaken at room temperature for 6 h. It was then rinsed with DMF–TEA, dried, and replaced on the synthesizer. Routine synthesis was resumed until the desired oligodeoxynucleotide was synthesized. A series of FPA-labeled ODNs were synthesized in this manner (Table 1). FPA-labeled oligodeoxynucleotides were purified via reverse-phase HPLC; retention times for labeled and unlabeled ODNs differed by several minutes. Isolated yields of the labeled ODNs ranged from 20–42%.

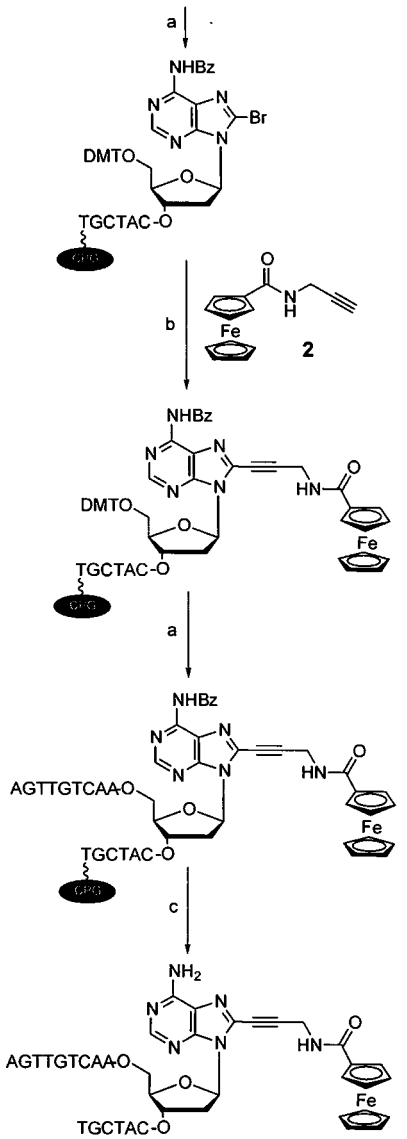


Key: (a) ODN synthesis; (b) $Pd(PPh_3)_4$, CuI, TEA, DMF; (c) ODN deprotection. Analogous procedure is used for 5-iodouridine modification.

Scheme 2. On-column synthesis of ferrocene-labeled oligodeoxynucleotides.

Table 1
Ferrocene-labeled oligodeoxynucleotides melting temperatures

| | Duplex | $T_m$ (°C) |
|---|---|---|
| Complementary | 5′-TGC TAC AAA CTG TTG A<br>3′-ACG ATG TTT GAC AAC T | 50.8 ± 0.3 |
| **1** | 5′-TGC TA*C AAA CTG TTG A<br>3′-ACG AT G TTT GAC AAC T | 43.2 ± 0.6 |
| **2** | 5′-TGC TAC A*AA CTG TTG A<br>3′-ACG ATG T TT GAC AAC T | 41.8 ± 0.9 |
| **3** | 5′-TGC TAC AAA* CTG TTG A<br>3′-ACG ATG TTT GAC AAC T | 42.4 ± 1.7 |
| **4** | 5′-TGC TAC AAA CTG TU*G A<br>3′-ACG ATG TTT GAC AA C T | 49.6 ± 0.1 |
| **5** | 5′-TGC TAC AAA CU*G TTG A<br>3′-ACG ATG TTT GA C AAC T | 48.2 ± 0.2 |

* = FPA.

Given that current automated DNA synthesis technology offers a convenient and high yielding procedure for synthesizing duplexes using phosphoramidites, we explored this second approach to ferrocene-labeled ODN. Three different ferrocene-phosphoramidites were synthesized as shown in Schemes 3 and 4. The ferrocene-uridine phosphoramidite (Scheme 3) was synthesized by coupling FPA, **2**, to 2′-deoxy-5′-dimethoxytrityl-5-iodouridine, **3**, in the presence of $Pd(PPh_3)_4$, CuI, and TEA (95% yield). Next, **4** was reacted with β-cyanoethylchloro-*N*,*N*-diisopropylphosphoramidite to afford the ferrocene-nucleoside phosphoramidite, **5**, which was column purified and used immediately for automated solid-phase DNA synthesis. The butanol derivatized ferrocene was synthesized as also shown in Scheme 3. Ferrocene monocarboxylic acid, **6**, was coupled to 1-(*t*-butyldiphenylsiloxy)-4-aminobutane using DCC (96% yield). The TBDPSi protecting group was then cleanly removed using TBAF in THF (95% yield). Finally, **7** was reacted with β - cyanoethylchloro - *N*,*N* - diisopropylphosphoramidite to afford the ferrocene-phosphoramidite, **8**, for 5′-terminal ODN labeling. Likewise, the 5-ferrocene labeled thymidine phosphoramidite, **14**, was prepared as shown in Scheme 4. First, the 5′-position of thymidine was converted from a hydroxyl to an amine in three consecutive steps. Thymidine, **9**, was treated with an equimolar amount of methanesulfonyl chloride in dry pyridine to afford **10** (55% yield) [50]. Next, the 5′-mesyl group was substituted with lithium azide to give **11** in 75% yield. Compound **11** was reduced with $H_2$ and Pd–C to give the 5′-amino-5′-deoxythymidine, **12** in 40% yield. Next, compound **13** was prepared by coupling ferrocene monocarboxylic acid, **6**, to 5′-amino-5′-deoxythymidine, **12**, in DMF using DCC (40% yield). Finally, **13** was reacted with β-cyanoethyl-*N*,*N*′-diisopropylchlorophosphoramidite in dry $CH_3CN$ to afford the ferrocene-phosphoramidite, **14**, ready for use in an oligodeoxynucleotide synthesizer.

All three ferrocene-phosphoramidites were incorporated in oligodeoxynucleotides during automated synthesis (Scheme 5) [52,53]. The syntheses were performed at the 1.0 μmol scale using the standard coupling protocol except that the ferrocene phosphoramidite step proceeded for 15 min to ensure sufficient coupling time. The sequences prepared were analogous to those prepared using the on-column approach. Once synthesized,

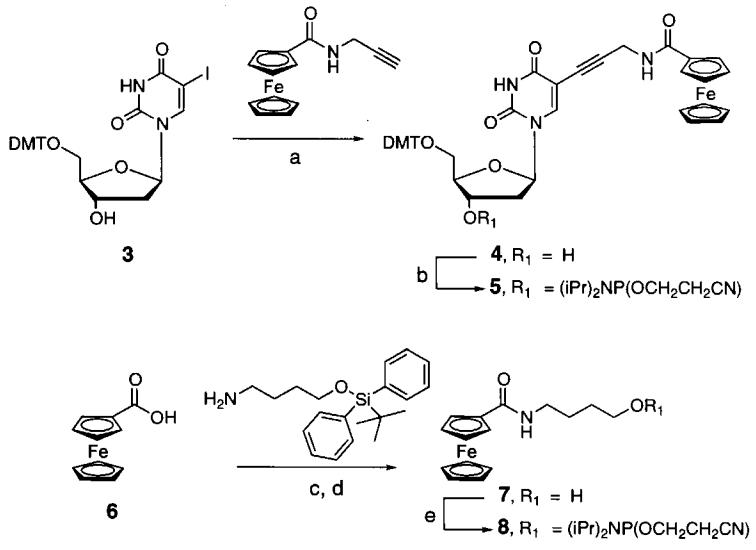


Key: (a) $Pd(PPh_3)_4$, CuI, TEA, DMF, 95% yield; (b) $ClP(iPr_2N)(OCH_2CH_2CN)$, DIPEA, $CH_3CN$, 86% yield; (c) DCC, HOBt, DIPEA, DMF, 96% yield; (d) TBAF, THF, 95% yield; (e) $ClP(iPr_2N)(OCH_2CH_2CN)$, DIPEA, $CH_3CN$, 95% yield.

Scheme 3. Synthesis of the ferrocene-uridine (**2**), and ferrocene butanol (**8**), phosphoramidites.

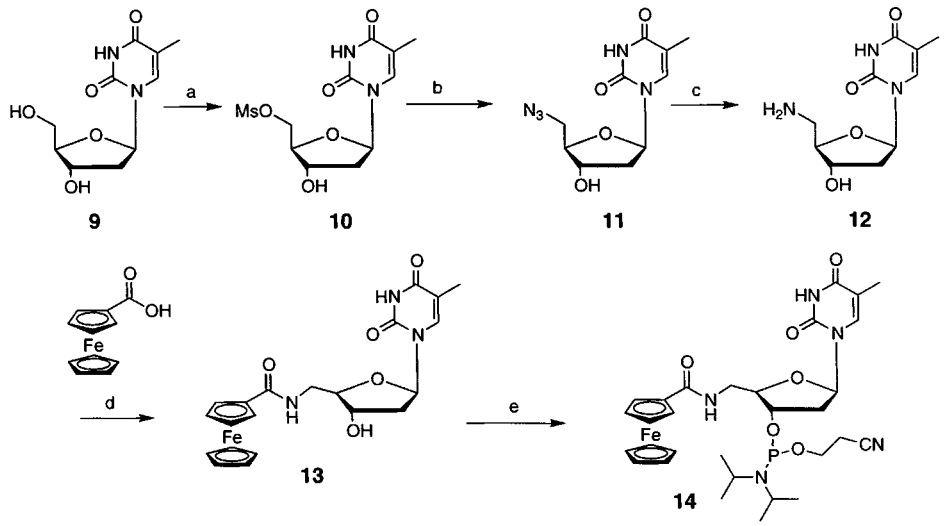


Scheme 4. Synthesis of the ferrocene-thymidine phosphoramidite (**14**).

the ferrocene-labeled oligodeoxynucleotides were cleaved from the column, and the exocyclic amines and phosphate groups were deprotected in 30% ammonium hydroxide. In all cases, these reactions yielded less material than the on-column approach. For the ferrocene phosphoramidites **5**, **8**, and **14**, the corresponding yields based on HPLC analysis of the labeled oligodeoxynucleotides were 10, 15 and 12%, respectively. With regards to the ferrocene-labeled oligodeoxynucleotides, the on-column approach gave consistently better yields of nucleobase labeled product and sufficient amounts of material for further study.

Before characterizing the ferrocene labeled ODNs, the spectroscopic properties of derivatized ferrocene compounds were first examined. For complete analysis, the FPA labeled analogues 2′-deoxyuridine and 2′-deoxyadenosine were also synthesized by coupling FPA to either 2′-deoxy-3′,5′-dibenzoyl-5-iodouridine or 8-bromo-2′-deoxyadenosine using the Pd(0)–CuI catalyst, to give $U^{FPA}$ (**15**) and $A^{FPA}$ (**16**), respectively (shown in Fig. 1). The UV–vis transitions of ferrocene, **2**, **7**, **13**, **15**, and **16**, are summarized in Table 2. All of the compounds display the characteristic weak (d–d) transition centered around 440 nm (ranging from 423 to 450 nm in the various derivatives). The molar absortivities increase slightly with attachment to the propargyl group. This weak optical transition is buried in the spectrum of the ferrocene-labeled oligodeoxynucleotide, which is dominated by the π–π* transition at 260 nm.

Cyclic voltammograms of **2**, **7**, **13**, **15**, and **16** in dichloromethane, revealed reversible oxidation with $E_{1/2}$ shifted positive 140–160 mV of ferrocene. This positive shift in potential is expected based on previous work [45]. As shown in Table 3, compounds **2**, **15**, and **16**, all with propargylamide linkages, have similar $E_{1/2}$ values near 50 mV. Compounds **7** and **13**, which contain amide linkages without the propargyl group have slightly lower $E_{1/2}$ values of 24 and 29 mV, respectively.

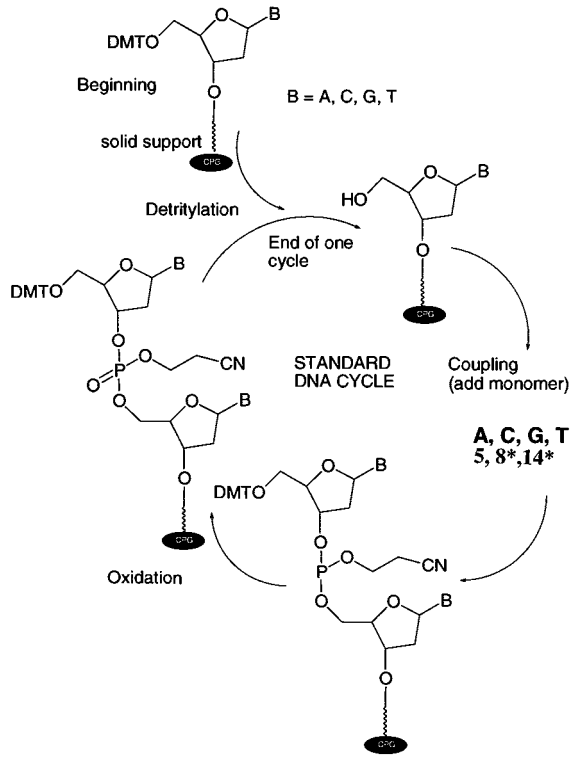


Scheme 5. Conventional solid-phase synthesis using ferrocene phosphoramidites. (*Compounds **8** and **14** can only be used to label the 5′-terminus of the oligodeoxynucleotide.).

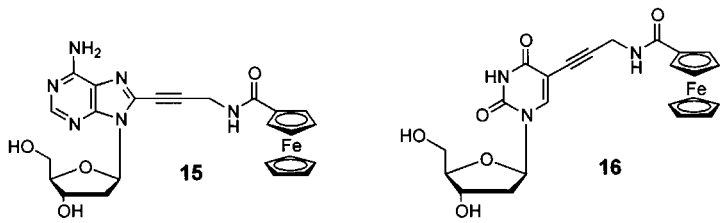


Fig. 1. Ferrocenoyl-propargylamide-2′-deoxyadenosine (**15**), and ferrocenoyl-propargylamide-2′-deoxyuridine (**16**).

Melting temperatures of $U^{FPA}$ labeled duplexes are only slightly lower than those of unmodified analogous strands, suggesting that the ferrocene label does not significantly decrease the stability of the duplex (Table 1). $T_m$ values for the labeled A strands are lower than those of the U-labeled strands, indicating that the introduction of $A^{FPA}$ in the duplex does disrupt base pairing to some extent. However, circular dichroism spectroscopy of the ferrocene-labeled duplexes indicate B-form structure for both the $A^{FPA}$ and $U^{FPA}$ labeled strands, as well as the unlabeled duplex, as shown in Fig. 2.

Table 2
UV–vis spectra data for the derivatized ferrocene compounds

| Compound | $\lambda_{max}$ nm ($\varepsilon$, $M^{-1}\,cm^{-1}$) |
|---|---|
| Ferrocene | 440 (142) |
| **2**, FPA | 450 (355) |
| **7** | 440 (246) |
| **13** | 440 (154) |
| **15**, $U^{FPA}$ | 423 (739) |
| **16**, $A^{FPA}$ | 430 (554) |

Table 3
Electrochemical data for the derivatized ferrocene compounds

| Compound | $E_{1/2}$ mV versus $Ag\,|\,Ag^+$ |
|---|---|
| Ferrocene | −114 |
| **2**, FPA | 50 |
| **7** | 24 |
| **13** | 29 |
| **15**, $U^{FPA}$ | 43 |
| **16**, $A^{FPA}$ | 48 |

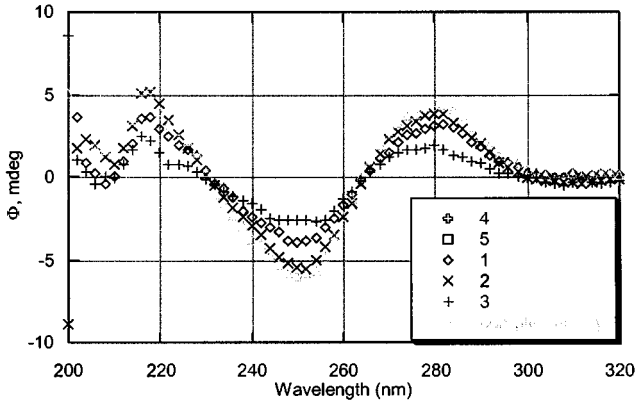


Fig. 2. CD spectra of ferrocene labeled and unlabeled oligodeoxynucleotide duplexes.

## 4. Conclusions

This study explores methods to covalently link ferrocene in close proximity to DNA without disrupting the overall DNA structure or interfering with Watson–Crick base-pairing selectivity. Specifically, on-column derivatization and phosphoramidite synthetic routes are evaluated. While we and others [39,40] are able to incorporate a ferrocene label at the 5′-terminus via the phosphoramidite approach, this method is best suited for use with a derivatized ferrocene containing longer alkyl chain spacers. For labeling at the nucleobase, the on-column approach is preferred. The ferrocene-labeled oligodeoxynucleotides reported herein form stable B-form duplexes with similar melting temperatures and CD spectra to the unlabeled analogues. In summary, this facile on-column procedure yields ODNs labeled site-specifically at the C5 position of 2′-deoxyuridine and the C8 position of 2′-deoxyadenosine with ferrocene. These ferrocene-labeled oligodeoxynucleotides are likely to be of use for studying DNA-mediated charge transfer and developing novel DNA diagnostic technologies.

## 5. Supplementary material

Supplementary Material is available from the author upon request: e-mail: mwg@chem.duke.edu. Website: http://www.chem.duke.edu/ ~ mwg/labgroup.

## Acknowledgements

This work was supported in part by the Army Office of Research and Glen Research. M.W.G. also thanks the Pew Foundation for a Pew Scholar in the Biomedical Sciences, the Alfred P. Sloan Foundation for a Research Fellowship, and the Dreyfus Foundation for a Camille Dreyfus Teacher Scholar.

## References


[1] G.B. Dreyer, P.B. Dervan, Biochemistry 82 (1985) 968.
[2] R. Manchanda, S.U. Dunham, S.J. Lippard, J. Am. Chem. Soc. 118 (1996) 5144.
[3] J. Schliepe, U. Berghoff, B. Lippert, D. Cech, Angew. Chem. Int. Ed. Engl. 35 (1996) 646.
[4] P.G. Sammes, G. Yahioglu, Nat. Prod. Rep. (1996) 1.
[5] D.S. Sigman, Acc. Chem. Res. 19 (1986) 180.
[6] A.E. Beilstein, M.T. Tierney, M.W. Grinstaff, Comments on Inorg. Chem. 22 (2000) 103.
[7] R.E. Holmlin, P.J. Dandliker, J.K. Barton, Angew. Chem. Int. Ed. Engl. 36 (1997) 2714.
[8] G.B. Schuster, Acc. Chem. Res. 33 (2000) 253.
[9] S.O. Kelley, J.K. Barton, in: S.O. Kelley, J.K. Barton (Eds.), Radical Migration Through the DNA Helix: Chemistry at a Distance, vol. 36, Marcel Dekker, New York, 1999, p. 211.
[10] T.L. Netzel, J. Biol. Inorg. Chem. 3 (1998) 210.
[11] M. Ratner, Nature 397 (1999) 480.
[12] U. Diederichsen, Angew. Chem. Int. Ed. Engl. 36 (1997) 2317.
[13] T.L. Netzel, in: T.L. Netzel (Ed.), A Comparison of Experimental and Theoretical Studies of Electron Transfer Within DNA Duplexes, Marcel Dekker, New York, 1998, pp. 1–54.
[14] M.W. Grinstaff, Angew. Chem. Int. Ed. Engl. 38 (1999) 3629.
[15] C.J. Murphy, M.R. Arkin, Y. Jenkins, N.D. Ghatlia, S.H. Bossmann, N.J. Turro, J.K. Barton, Science 262 (1993) 1025.
[16] D.B. Hall, R.E. Holmlin, J.K. Barton, Nature 382 (1996) 731.
[17] F.D. Lewis, R. Wu, Y. Zhang, R.L. Letsinger, S.R. Greenfield, M.R. Wasielewski, Science 277 (1997) 673.
[18] E. Meggers, M.E. Michel-Beyerle, B. Giese, J. Am. Chem. Soc. 120 (1998) 12950.
[19] E. Meggers, D. Kusch, M. Spichty, U. Wille, B. Giese, Angew. Chem. Int. Ed. Engl. 37 (1998) 460.
[20] P.T. Henderson, D. Jones, G. Hampikian, Y. Kan, G.B. Schuster, Proc. Natl. Acad. Sci. 96 (1998) 8353.
[21] D. Ly, Y. Kan, B. Armitage, G.B. Schuster, J. Am. Chem. Soc. 118 (1996) 8747.
[22] S.M. Waybright, C.P. Singleton, J.M. Tour, C.J. Murphy, U.H.F. Bunz, Organometallics 19 (2000) 368.
[23] G.H. Keller, M.M. Manak, DNA Probes, Stockton Press, New York, 1993.
[24] T.J. Meade, J.F. Kayyem, Angew. Chem. Int. Ed. Engl. 34 (1995) 352.
[25] X. Hu, G.D. Smith, M. Sykora, M.W. Grinstaff, Inorg. Chem. 39 (2000) 2500.
[26] W. Bannwarth, D. Schmidt, Tetrahedron Lett. 30 (1989) 1513.
[27] S.M. Gasper, G.B. Schuster, J. Am. Chem. Soc. 119 (1997) 12762.
[28] E.R. Holmlin, P.J. Dandliker, J.K. Barton, Bioconjugate Chem. 10 (1999) 1122.
[29] S.I. Khan, A.E. Beilstein, M. Sykora, G.D. Smith, X. Hu, M.W. Grinstaff, Inorg. Chem. 38 (1999) 3922.
[30] M.T. Tierney, M.W. Grinstaff, J. Org. Chem. 65 (2000) 5355.
[31] J. Telser, K.A. Cruickshank, K.S. Schanze, T.L. Netzel, J. Am. Chem. Soc. 111 (1989) 7221.
[32] J.D. Kahl, M.M. Greenberg, J. Am. Chem. Soc. 121 (1999) 597.
[33] D.J. Hurley, Y. Tor, J. Am. Chem. Soc. 120 (1998) 2194.
[34] S.I. Khan, A.E. Beilstein, M.W. Grinstaff, Inorg. Chem. 38 (1999) 418.
[35] S.I. Khan, M.W. Grinstaff, J. Am. Chem. Soc. 121 (1999) 4704.
[36] S.I. Khan, A.E. Beilstein, M.T. Tierney, M. Sykora, M.W. Grinstaff, Inorg. Chem. 38 (1999) 5999.
[37] A.E. Beilstein, M.W. Grinstaff, Chem. Commun. (2000) 509.
[38] M.T. Tierney, M.W. Grinstaff, Org. Lett. 2 (2000) 3413.
[39] R.C. Mucic, M.K. Herrlein, C.A. Mirkin, L. Letsinger, Chem. Commun. (1996) 555.
[40] T. Ihara, M. Nakayama, M. Murata, K. Nakano, M. Maeda, Chem. Commun. (1997) 1609.
[41] C.J. Yu, H. Yowanto, Y. Wan, T.J. Meade, Y. Chong, M. Strong, L.H. Donilon, J.F. Kayyem, M. Gozin, G.F. Blackburn, J. Am. Chem. Soc. 122 (2000) 6767.
[42] S. Takenaka, Y. Uto, J. Saita, M. Yokoyama, H. Kondo, W.D. Wilson, Chem. Commun. (1998) 1111.
[43] A. Hess, N. Metzler-Nolte, Chem. Chem. (1999) 885.
[44] J.C. Verheijen, G.A. van der Marel, J.H. van Boom, N. Metzler-Nolte, Bioconjugate Chem. 11 (2000) 741.
[45] H.B. Kraatz, J. Lusztyk, G.D. Enright, Inorg. Chem. 36 (1997) 2400.
[46] K. Severin, R. Bergs, W. Beck, Angew. Chem. Int. Ed. Engl. 37 (1998) 1634.
[47] O. Brosch, T. Weyhermuller, N. Metzler-Nolte, Eur. J. Inorg. Chem. (2000) 323.
[48] K. Sonogashira, Y. Tohda, N. Hagihara, Tetrahedron Lett. 50 (1975) 4467.
[49] M. Wießler, D. Schütte, Preparation of Metallocene-phosphoramidite Conjugates for use in Electron-microscope Visulaization of DNA or RNA. In: M. Wießler, D. Schütte (Ed.), Germany, 1996, p. 8.
[50] J.R. Horwitz, J. Chua, M. Noel, J. Org. Chem. 29 (1964) 2076.
[51] J.D. Watson, F.H. Crick, Nature 171 (1953) 737.
[52] M.H. Caruthers, Acc. Chem. Res. 24 (1991) 284.
[53] M.J. Gait, Oligonucleotide Synthesis: A Practical Approach, IRL Press, Washington, DC, 1984.